REAL-TIME SAR SIMULATION FOR CHANGE DETECTION APPLICATIONS BASED ON DATA FUSION

Timo Balz

Institute for Photogrammetry (ifp), Universität Stuttgart, Germany
Geschwister-Scholl-Strasse 24D, D-70174 Stuttgart
timo.balz@ifp.uni-stuttgart.de

Commission II WG 1, Commission VII WG 6 & 7

KEY WORDS: SAR, Real-time, Simulation, Change Detection, Fusion

ABSTRACT:

SAR simulators are important tools for developing new SAR systems as well as for supporting the analysis of acquired SAR data. Using modern graphics cards for SAR simulation, even complex environments can be simulated in real-time. This is realized by implementing SAR geometry and radiometry within standard graphics hardware, which nowadays offers 3D hardware acceleration and programmable graphics processing units (GPU). The geometric differences between optical and SAR images are the biggest challenge for any multi-sensor data fusion approach. High-resolution data fusion should be based on 3D models, in urban areas provided by city models. Differences between the model and the newly acquired data can be detected by comparing the simulation of the data with the acquired data. Due to unreliable models and inaccurate simulation results, automatic approaches provide various false alarms. Semi-automatic approaches are more reliable alternatives.

1. INTRODUCTION

The time needed to calculate a SAR simulation is not crucial for most scientific applications or for applications in sensor design. For these applications, the SAR simulation has to be as realistic as possible. A totally different application scenario is the real-time visualization of SAR effects. Here the realism of the simulation is not crucial, but the visualization must be in real-time. Real-time SAR simulations are useful for interactive applications, like mission planning or applications in training and education. Furthermore, simulation assisted change detection and data fusion benefit from simulation results in real-time.

Radar images differ in many ways from images acquired by passive sensor systems. Any data fusion approach has to consider these differences. The combination of SAR simulation and visualization provides new methods for model based data fusion. Based on 3D models, e.g. city models, differences between the model and the newly acquired data can be detected by comparing the simulation of the models with the acquired data. Data fusion between high-resolution SAR and optical images must consider the terrain and the 3D shape of the objects of interest. Fusing an agricultural area for vegetation classification in a low resolution, the topography of the area is negligible. Using high-resolution images in mountainous or urban areas, the terrain and object shapes have to be taken into consideration. This requires 3D models of the area of interest. Beside the problem of availability, the quality and reliability of these models is often questionable. Any change detection based on such models has to be aware of this problem and has to accept the incompleteness of the models as well as the inaccuracies of the physical models or of the simplified implementation used for the simulation. Semi-automatic approaches are reliable alternatives.

In the following section, the development of the graphics hardware is briefly discussed. In section 3, the real-time SAR simulation tool SARViz will be presented. While in section 4 the need for 3D shape awareness in data fusion is discussed. Fusion based change detection in urban areas will be demonstrated in the final part of the paper.

2. GENERAL-PURPOSE COMPUTATION ON GRAPHICS PROCESSING UNITS

Rapid developments in computer graphics allow for more and more realistic visualization of extensive virtual worlds in real-time. Visualization applications are realized by GPUs. A modern GPU is a data-parallel streaming processor working in a single-instruction, multiple data (SIMD) fashion. Because GPUs are highly parallel and specialized on certain arithmetic operations, these operations can be calculated astonishingly fast. As depicted in Figure 1, GPUs of the latest generation have more computational power as standard CPUs, providing nowadays almost supercomputing speed.

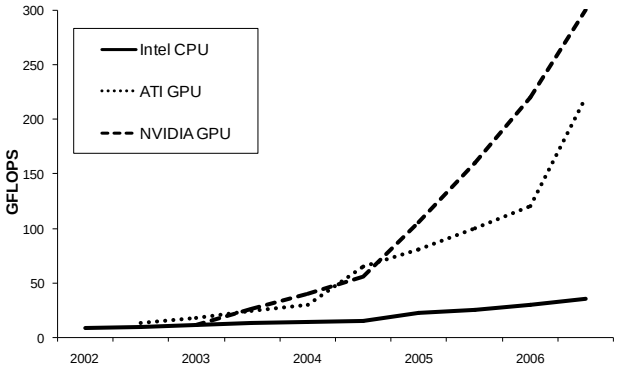

Figure 1. Comparison between CPU and GPU speed (see Buck, 2004; Owens et al, 2007)

Beside visualization, the programmable graphics hardware can also be used for a variety of general-purpose computations (Owens et al, 2007). A GPU design differs from a CPU design. As shown in Figure 2, a big part of the CPU is used for branching, whereas most transistors on the GPU are used for arithmetic operations (Owens, 2005).

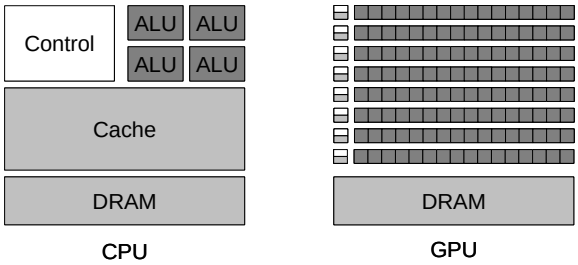

Figure 2. A GPU uses more transistors as arithmetic logical units (NVIDIA, 2007)

In rasterization, each geometry primitive is calculated separately from the others, which allows for a highly parallel design. The visualization is controlled by the so-called graphics pipeline (see Figure 3). After the transformation from world to screen space, calculated by the so-called vertex shader, the data is rasterized by the hardware rasterizer of the graphics card. Each resulting pixel is piped through the pixel shader, another specialized and programmable part of today's graphics hardware. The pixel shader is used to compute the color of each displayed pixel. This is done according to the lighting and material or texture information of each pixel. Due to the flexible and programmable shaders used in modern graphics cards, different methods for calculating the reflections can be implemented. Finally, the so called z-buffering is done before the image is displayed on the screen or saved in the texture memory of the graphics hardware.

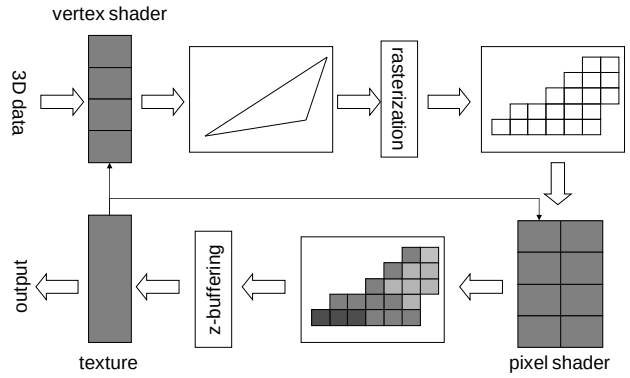

Figure 3. Programmable graphics pipeline of modern graphics cards

SAR simulations are visualization applications. GPUs are therefore well suited for SAR simulations. But radar images differ in many ways from images acquired by passive sensor systems. Using the flexible programmable GPUs, the different imaging geometry and radiometry of radar images can be implemented, as described in the following section.

3. REAL-TIME SAR SIMULATION USING SARVIZ 1.0

The real-time SAR simulation tool SARViz (Balz, 2006), has been constantly improved since it has been presented for the first time in 2006. The newest version is supporting squint angles, real multi-look, the visualization of moving objects as well as simple bi-static configurations. SARViz is using methods developed by computer graphics to simulate SAR images. The GPU is processing triangles using local illumination. Each triangle is visualized independently from the other triangles. Each triangle point is processed by the vertex shader, which treats the geometry. After the rasterization, the radiometry of each pixel is calculated by the pixel or fragment shader.

3.1 SAR geometry

The vertex shader is transforming each point from the model coordinate system to world coordinates and then subsequently to image coordinates. The so-called camera transformation matrix (Microsoft, 2005) has to be adapted to achieve the desired parallel projection.

The range position of each object in a SAR image depends on the distance between the object and the sensor, thus higher points, i.e. points with larger *z*-values, are closer to the sensor and are therefore mapped closer to near-range. The resulting shift in range direction Δx, depends on the height above the ground level *z* and the off-nadir angle θ_{off} :

$$\Delta x = z \cdot \tan(\theta_{off})$$

3.2 SAR radiometry

The pixel shader is processing every pixel to compute the corresponding radiometry. For each pixel the corresponding face normal is determined using a 3D model. Taking material properties, like the dielectric constant, and sensor properties into account, the reflection strength can be calculated. SARViz offers three different methods of backscattering computation. The statistical method based on measurements of Ulaby & Dobson (1989), a direct calculation based on the roughness and dielectric constant of the material developed by Zribi (2006) and an adaptation of computer graphics methods. Most commonly used is the adaptation of the computer graphics methods, due to its computing time efficiency.

According to the Phong reflection model (Phong, 1975), three illumination elements (diffuse, specular and ambient) are combined. In computer graphics, the diffuse element is calculated using the material properties and the light strength as well as the light position and face normal $\vec{n}$ (Gray, 2003). In the SAR case, the reflection strength is determined by the reflections strength *r* and the sensor position vector $\vec{s}$:

$$\sigma_d = r\langle \vec{n}, \vec{s} \rangle$$

The specular part of the overall reflection value can be derived from the visualization of optical specular reflections based on Blinn's (1977) work, with $p \approx 32$. Because in the mono-static SAR case the "light" and "camera" position are identical, the calculation can be simplified:

$$\sigma_s = r\langle \vec{n}, \vec{s} \rangle^p$$

Comparing the calculated results with the statistical analysis of Ulaby & Dobson, it is possible to retrieve realistic values for the reflection and the roughness values, which are needed to calculate the overall reflection strength.

The reflection is calculated locally. Therefore, multi-reflections as well as shadows are not supported. In the rasterization approach, the paths of the rays are not traced and every vertex and pixel is processed separately, therefore occlusions are not modeled. By using shadow maps (Williams, 1978) both shadows and occluded areas can be modeled. A shadow map is generated in two steps. First, the scene is rendered from the position of the light source, which is in the mono-static case equivalent to the SAR sensor position. Instead of reflection values, the distance of every rendered pixel to the sensor is written to the so-called shadow map, as it is depicted in Figure 4.

In the second step the scene is rendered from the position of the virtual camera. SARViz directly simulates ground-range images to avoid the computational intense transformation from slant-range to ground-range. Because of this, the scene is rendered

looking from nadir direction, keeping a parallel projection. The distance of each pixel rendered in the nadir view is compared to the transformed distance between the sensor position and the object. If the distance of a pixel to the sensor exceeds the value stored in the shadow map, the pixel is not visible and will not be rendered.

Figure 4. SAR shadow map generation

Shadow mapping is an image-based technique. It can be easily implemented and generates fast shadow casting effects. Using this method, the virtual camera is not allowed to be inside a shadow area. Large distance differences between the virtual camera and the light source are also problematic. For mono-static SAR simulation, the sensor is identical to the light source and the virtual camera. Therefore, no such problems exist. Still, precision and aliasing problems may occur while using shadow maps.

3.3 Soft shadows

The edges of a shadow area created by shadow mapping are too sharp, because each pixel is either completely inside or outside of a shadow area. In computer graphics various methods for visualizing soft shadows are used. Optical images have very soft shadows, especially if they include ambient lighting. In radar images, there is no ambient lighting. The methods visualizing ambient light are therefore not feasible for SAR simulation.
Due to the shape of the radar lobe, areas in the edge of the shadow still reflect energy back to the sensor. This can be visualized by generating three shadow maps. One shadow map in the image centre using parallel projection, two shadow maps at the edges of the image. The positions of these additional shadow maps are determined by the shape of the radar lobe, which depends on the length of the real aperture. Using three shadow maps, the shadow state of a pixel is not binary anymore.
In our approach we differentiate between pixels outside any shadow area, pixels inside one shadow area and pixels inside two or more shadow areas. Pixels inside two or more shadow areas are not reflecting any energy back to the sensor, but the pixels inside just one of the shadow areas are still reflecting a limited amount of energy back to the sensor. As it can be seen in Figure 5, this approach is considering the shape of the radar lobe and is visualizing soft radar shadows.

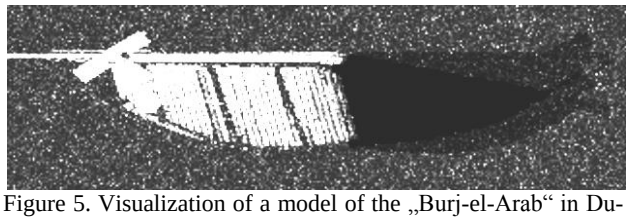
Figure 5. Visualization of a model of the „Burj-el-Arab“ in Dubai using soft shadows

3.4 Spotlight mode

The spatial resolution of SAR systems can be increased using the spotlight mode. In the spotlight mode the squint angle of the radar antenna is adjusted during the data acquisition to increase the exposure time. The dynamic adjustment of the antenna increases the synthetic aperture length and therefore improves the spatial resolution in azimuth.

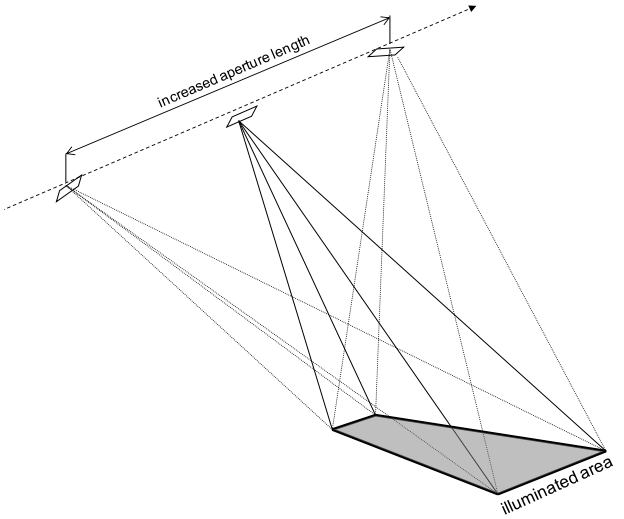

Figure 6. SAR spotlight mode

Beside the improvement of the resolution, the spotlight mode influences the lighting, the shadow casting and the layover effect. To visualize the influence of the spotlight mode on the layover, the geometry is adjusted dynamically in the vertex shader. The shadow is calculated using three shadow maps. In contrast to the visualization of soft shadows, explained in section 3.3, the shadow of each pixel is determined by using only one shadow map. Depending on the azimuth position, the respective shadow map is selected. Therefore, the shadow map used for the shadow calculation is dynamically changing.

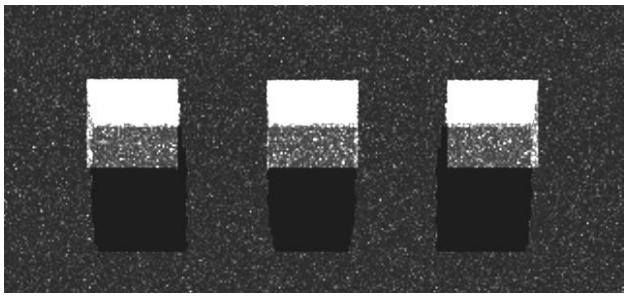
Figure 7. Visualization of three simple buildings using the spotlight mode

3.5 Speckling and multi-look image generation

Speckling is produced by mutual interference of coherent waves that are subject to phase differences. For simplicity it can be visualized by additive noise. The reflection value of a multi-look image is a combination of *m* single SAR images. The resulting speckle value in a multi-look image S_m can be calculated using:

$$S_m = \frac{1}{m}\sum_{i=1}^{m} S_i$$

A more realistic approach is the separate simulation of each look. Each sub-aperture image has a different squint angle. Although the differences between the squint angles are small, edges, layovers and shadows appear blurred in the combined multi-look image (see Figure 8). Because each single sub-aperture image has to be simulated separately, the overall processing time increases accordingly.

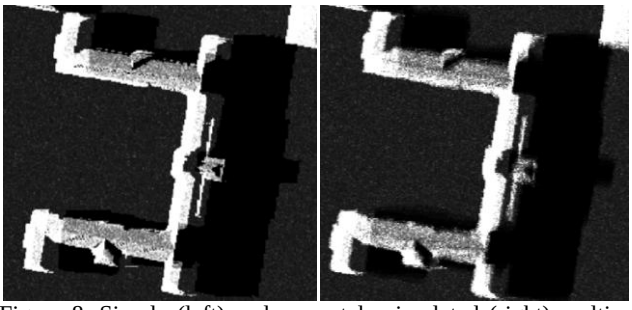

Figure 8. Simple (left) and separately simulated (right) multi-look image of the New Palace (Neues Schloss) in Stuttgart

3.6 Side-lobe visualization

Strong reflecting objects like corner reflectors can cause typical blooming effects in SAR images. The blooming is caused by the high amount of energy reflected back to the sensor. Analyzing the simulation result, which is first rendered to a texture, strong reflections are detected. Depending on a certain threshold, reflections are considered to cast side-lobes. Afterwards these side-lobes are additively rendered to the simulation result, as depicted in Figure 9.

Figure 9. SARViz simulation of the 3D-model of the „Stiftskirche“ in Stuttgart

4. IMAGING GEOMETRY AWARE DATA FUSION

Fusing SAR data and optical imagery can provide a variety of new information, not available analyzing each data set separately. Using low or medium resolution data, the data fusion can be done by simple methods. In flat terrains, even straightforward geo-coding approaches are suitable. While analyzing vegetation in images with about 25m ground resolution, the different geometries of the images are not crucial, because the layover of most vegetation related objects is influencing less than one pixel.

But while analyzing today’s high-resolution images, this is not true anymore. The spatial resolution of SAR sensors improved tremendously during the last decade. The new TerraSAR-X provides images with a spatial resolution of about one meter (Werninghaus, 2006), modern airborne systems achieve spatial resolutions in the decimeter scale (Ender & Brenner, 2003). In these images, the geometrical effects caused by the distance geometry of a SAR image are significant, especially in urban areas. The appearance of buildings in high-resolution images differs from the low-resolution appearance. Even small structures are visible inside the layover.

The position, the shape and the radiometric appearance of any object depends on the sensor position, the sensor properties and the environment of the object. For a successful fusion of high-resolution images from different sensor types, the sensor properties as well as the 3D shape of the objects of interest should be known. The spatial accuracy of this data has to be high, because for any data fusion approach, the geo-coding accuracy should match the data resolution (Soergel et al, 2006). If the shape is available, additional information about the object properties can be analyzed. Analyzing bridges for example, the outlines of a bridge can be easily determined using aerial photos, whereas deriving the outlines using SAR is difficult. Using the width from the aerial image measurement and the true position of the bridge from the double-bounce reflection, the real height of the bridge can be determined easily (Soergel et al, 2007). For many applications such approaches are not feasible. Remote sensing is often used because the terrain and the objects are unknown. Any remote sensing approach considering information about the 3D terrain or shape as prerequisites is problematic.

Multi-sensor data fusion can be implemented as a multi-step strategy. The chosen strategy depends on the application and the available data. Assuming no change in the terrain or the 3D shape between the different images, e.g. because the time difference between the acquisitions is small, the 3D shape of the area can be determined by one sensor and the data fusion is based on the generated model. The 3D model can be generated by standard remote sensing methods like interferometric SAR, LIDAR or photogrammetry (Brenner, 2005). Also terrestrial data acquisition by terrestrial laser scanning, photogrammetry or video-based reconstruction (Mordohai et al, 2007) is possible. Further research could reveal a path for a direct generation of 3D models from optical and SAR images, but this has not yet been presented. In another approach, changes occurring between the image acquisition times are assumed. In this case, the 3D shape should be generated from the data acquired earlier. Changes which occur between the acquisition dates can be detected based on the fusion of the data.

5. SAR SIMULATION ASSISTED CHANGE DETECTION

Assuming available stereo images, LIDAR or terrestrial data, 3D building models can be generated. The automated generation of building models using LIDAR and GIS footprint information is a well-known approach (Haala & Brenner, 1999). The building models in Figure 11 are reconstructed using this automated method. Like any automated approach, some models are not reconstructed correctly.

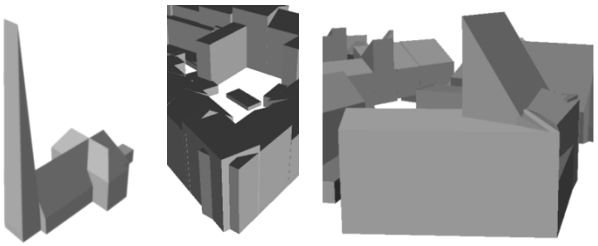

Figure 10. Erroneous reconstructed building models

If this erroneous reconstructed models are used for change detection applications, various false alarms will occur.

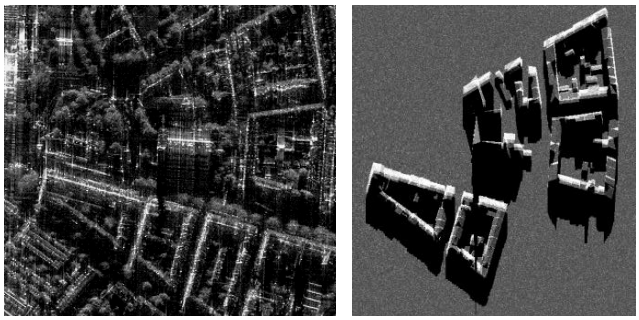

Figure 11. Subset of a DOSAR image of Karlsruhe (left) and SARViz simulation of the area (right)

In Figure 11 the real DOSAR image and the SARViz simulation of the erroneously reconstructed test area are depicted. DOSAR is the multi-frequency polarimetric airborne SAR system of the EADS Dornier GmbH (Hoffmann & Fischer, 2002). The off-nadir angle is 70° and the 3dB-resolution is about 0.57m. For testing purposes an artificially changed model, depicted in Figure 12, has been used. The black building has been added to the model to test the proposed change detection algorithm.

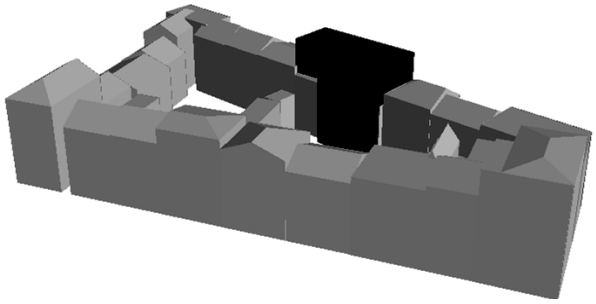

Figure 12. Changed 3D model

The detected changes are visible in Figure 13. Not only the changes from the artificially inserted house are visible, but additionally some changes in the centre of the building block are visible and even larger differences are detected in the south-east corner of the building block. These changes are directly related to the incomplete and erroneous city model illustrated in Figure 10.

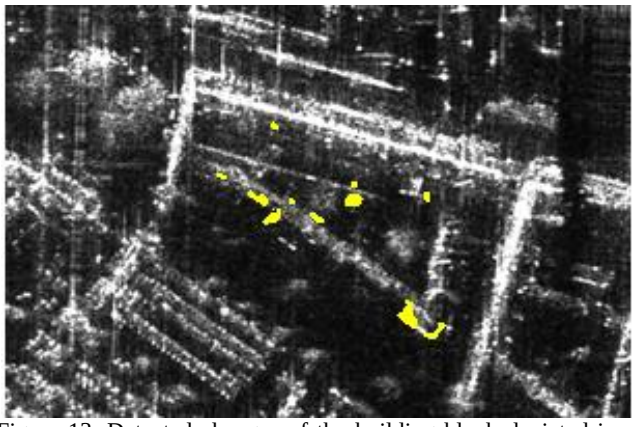

Figure 13. Detected changes of the building block depicted in Figure 12 overlaying a DOSAR image

As already presented before (Balz, 2004), the false alarms are outweighing the detected changes. For automated change detection based on simulation assisted fusion of automatically generated 3D data, the building reconstruction process is crucial.
More reliable building models can be reconstructed using semi-automatic reconstruction systems. The "CyberCity Modeler" published by Grün and Wang (1998) is commercially available. Using the semi-automated reconstruction the false alarms based on wrongly reconstructed models will be reduced. Due to generalizations in the reconstruction process and objects which are not included in the reconstructed building models, e.g. trees or parking cars, still various false alarms will occur.
Semi-automated change detection or alarm verification processes are another way of reducing false alarms. Assumed changes can be presented together with the model and the real image, clarifying the reason for the assumed change. Errors in the building model as well as possible false detections due to the object environment can be analyzed fast and reliable by human interpretation.

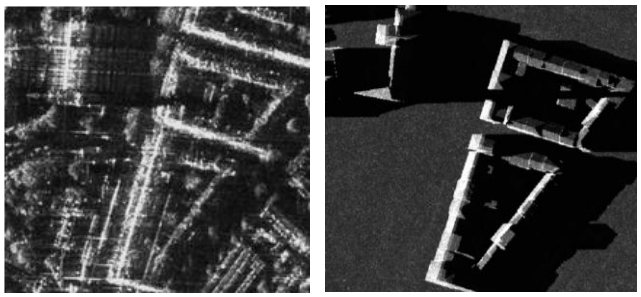

Figure 14. Original DOSAR image (left) and SARViz simulation (right) of the modified 3D model from Figure 12.

Comparing the real image and the simulation separately, errors and changes are not easily recognizable. For example in Figure 14, the erroneous building added to the model cannot be found easily. In Figure 15, the simulation is overlaying the real SAR image in real-time. The transparency is selectable and the simulation parameters can be changed at any time. Using this way of data visualization, changes can be detected easily and reliably.

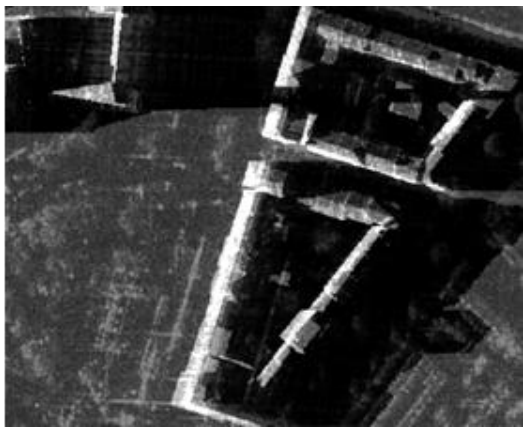

Figure 15. SAR image overlaid by a SARViz simulation

Changes and effects of assumed changes on the acquired SAR or optical image can be analyzed in real-time using visualization applications. False alarms due to erroneous building models can be detected, for example, by visually comparing aerial images of the area overlaid by computer visualizations of the building models. This way of false alarm detection and quality control is depicted in Figure 16.

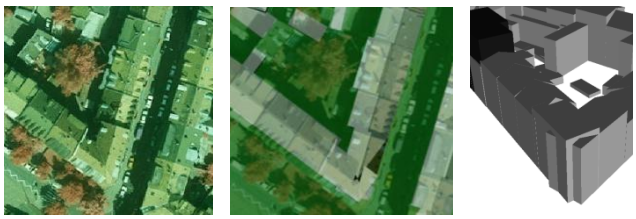

Figure 16. Comparison of the aerial image (left) the image overlaid by the model (middle) and the oblique view of the building model (right)

Interactive and simulation based change detection is a reliable way of analyzing SAR data in urban areas. Beside the detection of changes, the dimension of the change can even be measured by interactively adapting the shape of the model and visually comparing the simulation of the adapted model and the real SAR image. Thanks to the real-time simulation capability, this can be done fast and user-friendly.

6. CONCLUSION

New applications can be developed by using the power of modern GPUs for SAR simulation purposes. Interactive applications need real-time simulators. Especially applications in education, mission planning and interactive image analysis depend on real-time simulation results. Nowadays, this is possible even using low-cost hardware and software solutions.
The real-time simulator SARViz simulates a wide variety of different SAR configurations. Using the programmable shaders of modern GPUs, SAR images can be visualized as fast as scenes in modern computer games. As well as computer graphics visualizations get more and more complex and realistic, the SAR simulation can benefit from these developments by simulating more and more complex scenes faster and faster. Although the real-time simulation is not providing as realistic results as other SAR simulators, for a variety of applications the results are suitable.
High-resolution data fusion between optical and radar images must consider the terrain and the shape of objects of interest. Change detection based on the fusion of different data sets can be assisted by simulations. Mainly due to erroneous and incomplete 3D models, simulation assisted automatic change detection approaches suffer from high false-alarm rates. More reliable results can be expected using interactive change detection methods. SARViz can provide real-time SAR simulation of 3D models as well as optical visualizations of these models. Due to the possibility of combining different data sets, SARViz is a fast and reliable tool for image interpretation.

REFERENCES

Balz, T., 2004. SAR simulation based change detection with high-resolution SAR images in urban environments. In: *IAPRS Vol. 35, Part B*, Istanbul.

Balz, T., 2006. Real Time SAR-Simulation on Graphics Processing Units. In: *Proceedings of the 6th European Conference on Synthetic Aperture Radar (EUSAR 2006)*, Dresden.

Blinn, J.F., 1977. Models of light reflection for computer synthesized pictures. In: *Proceedings of the 4th annual conference on Computer graphics and interactive techniques (SIGGRAPH '77)*, San Jose.

Brenner, C., 2005. Building reconstruction from images and laser scanning. In: *International Journal of Applied Earth Observation and Geoinformation*, 6, pp. 187-198.

Buck, I., 2004. GPU computation strategies and tips. In: *Proceedings of the conference on SIGGRAPH 2004 course notes GRAPH '04*, Los Angeles.

Ender, J.H.G., Brenner, A.R., 2003. PAMIR - a wideband phased array SAR/MTI system. In: *IEE Proceedings - Radar, Sonar and Navigation*, 150 (3), pp. 165-172.

Gray, K., 2003. *Microsoft DirectX 9 Programmable Graphics Pipeline*. Microsoft Press, Redmond, Washington.

Grün, A., Wang, X., 1998. CC-Modeler: A Topology Generator for 3-D City Models. In: *ISPRS Journal of Photogrammetry & Remote Sensing*, 53, pp. 286-295.

Haala, N., Brenner, C., 1999. Extraction of buildings and trees in urban environments. In: *ISPRS Journal of Photogrammetry and Remote Sensing*, 54 (2-3), pp. 130-137.

Hoffmann, K., Fischer, P., 2002. DOSAR: A Multifrquency Polarimetric and Interferometric Airborne SAR-System. In: *2002 International Geoscience and Remote Sensing Symposium and the 24th Canadian Symposium on Remote Sensing*, Toronto.

Microsoft, 2005. DirectX 9.0c Software Development Kit. In: *http://www.microsoft.com/directx*

Mordohai, P., Frahm, J.-M., Akbarzadeh, A., Clipp, B., Engels, C., Gallup, D., Merrell, P., Salmi, C., Sinha, S., Talton, B., Wang, L., Yang, Q., Stewenius, H., Towles, H., Welch, G., Yang, R., Pollefeys, M., Nister, D., 2007. Real-time video-based reconstruction of urban environments. In: *Proceedings of the 2nd ISPRS International Workshop 3D-ARCH 2007: 3D Virtual Reconstruction and Visualization of Complex Architectures*, Zurich, Switzerland.

NVIDIA, 2007. CUDA Programming Guide Version 1.0. In: *http://developer.nvidia.com*

Owens, J.D., 2005. Streaming Architectures and Technology Trends. In: Pharr, M.: *GPU Gems 2. Programming Techniques for High-Performance Graphics and General-Purpose Computation*. Addison-Wesley, Boston, pp. 457-470.

Owens, J.D., Luebke, D., Govindaraju, N., Harris, M., Krüger, J., Lefohn, A.E., Purcell, T.J., 2007. A Survey of General-Purpose Computation on Graphics Hardware. In: *Computer Graphics Forum*, 26 (1), pp. 80-113.

Phong, B.T., 1975. Illumination for computer generated pictures. In: *Communications of the ACM*, 18 (6), pp. 311-317.

Soergel, U., Thiele, A., Cadario, E., Thoennessen, U., 2007. Fusion of high-resolution InSAR data and optical imagery in scenes with bridges over water for 3D visualization and interpretation. In: *Proceedings of the ISPRS VII WG2 & WG7 Conference on Information Extraction from SAR and Optical Data, with Emphasis on Developing Countries*, Istanbul, Turkey.

Soergel, U., Thoennessen, U., Brenner, A., Stilla, U., 2006. High-resolution SAR data: new opportunities and challenges for the analysis of urban areas. In: *IEE Proceedings - Radar, Sonar and Navigation*, 153 (3), pp. 294-300.

Ulaby, F.T., Dobson, M.C., 1989. *Handbook of Radar Scattering Statistics for Terrain*. Artech House, Norwood, Massachusetts.

Werninghaus, R., 2006. The TerraSAR-X Mission. In: *Proceedings of the 6th European Conference on Synthetic Aperture Radar (EUSAR 2006)*, Dresden.

Williams, L., 1978. Casting curved shadows on curved surfaces. In: *ACM SIGGRAPH Computer Graphics, Proceedings of the 5th annual conference on Computer graphics and interactive techniques SIGGRAPH '78*, Atlanta.

Zribi, M., Baghdadi, N., Guérin, C., 2006. A new Semi-empirical model for the analysis of surface roughness heterogenity. In: *Proceedings of the 2006 IEEE International Geoscience and Remote Sensing Symposium and 27th Canadian Symposium on Remote Sensing (IGARSS 2006)*, Denver, Colorado.